

# Electrophysiological Response of Cultured Trabecular Meshwork Cells to Synthetic Ion Channels

Pawel Fidzinski,<sup>1</sup> Andrea Knoll,<sup>2</sup> Rita Rosenthal,<sup>1</sup> Anna Schrey,<sup>2</sup> Andrea Vescovi,<sup>2</sup> Ulrich Koert,<sup>2,4</sup> Michael Wiederholt,<sup>1</sup> and Olaf Strauß<sup>3,\*</sup>

<sup>1</sup>Institut für Klinische Physiologie  
Universitätsklinikum Benjamin Franklin  
Freie Universität Berlin  
Hindenburgdamm 30  
12200 Berlin

<sup>2</sup>Institut für Chemie der Humboldt Universität zu Berlin  
Hessische Strasse 1-2  
10115 Berlin

<sup>3</sup>Universitätsklinikum Hamburg-Eppendorf  
Klinik und Poliklinik für Augenheilkunde  
Bereich Experimentelle Ophthalmologie  
Martinistrasse 52  
20246 Hamburg  
Germany

## Summary

The response of living cells of the trabecular meshwork to synthetic ion channels is described. The THF-gramicidin hybrids THF-gram and THF-gram-TBDPS as well as a linked gA-TBDPS and gramicidin A were applied to cultured ocular trabecular meshwork cells. THF-gram application (minimal concentration,  $10^{-8}$  M; saturation,  $10^{-7}$  M) led to an additional conductance which displayed characteristics of weak Eisenman-I selective cation channels, no cell destruction, an asymmetric change of the inward/outward currents, and higher current densities using  $\text{Cs}^+$  as charge carrier compared to  $\text{Na}^+$  and  $\text{K}^+$ . Linked-gA-TBDPS showed at  $10^{-12}$  M increases of the membrane conductance comparable to gA at  $10^{-7}$  M and a much faster response of the cells. Thus, THF-gramicidin hybrids form a basis for the use of synthetic ion channels in biological systems, which eventually may lead to new therapeutic approaches.

## Introduction

With the development of the patch-clamp technique, it became more and more clear that ion channels are involved in the regulation of nearly all cell functions [1, 2]. Several severe hereditary diseases which are caused by mutations in ion channel genes (channelopathies) show the medicinal relevance of ion channels [1]. In the recent past, substantial progress was made to correlate structure and function of biological ion channels [3, 4]. Additional understanding of ion channel function came from studies of synthetic ion channels in artificial membranes [5–11]. The investigation of synthetic ion channels in living cells is a nearly unexplored field [12]. This challenging task holds the potential to develop synthetic

ion channels as potential drugs to modulate cellular functions or to restore lacking ion channel activity.

We have chosen gramicidin A (gA) [5, 6] as a lead structure for ion channel design (Figure 1) [11, 13–17]. gA, a bacterial antibiotic, acts in planar lipid bilayers as a cation channel with a weak Eisenmann I selectivity [5]. Its active conformation, a  $\beta$ -helical head-to-head dimer, has a length in the range of the lipophilic part of the phospholipid bilayer. Due to specific interactions of the gA side chains with both the membrane interior and the membrane-water interface, this dimer is able to establish a membrane-spanning pore [6].

Our channel design is based on the covalent linkage [11, 17–19] of the gA motif and the incorporation of synthetic building blocks [13, 16, 20, 21], such as the *cis* tetrahydrofurane amino acid (H-THF-OH) [22], with the goal to tune the channel function. Thus, in synthetic THF-gram the hydrophobic valine-rich motif (residues 1–8) is replaced by a tetra-THF sequence [13]. Since monovalent cations show a high affinity to ether and polyether functionalities, the tetrahydrofurane moiety is supposed to interact with monovalent cations and influence the overall ion-conductance properties. Both N termini in THF-gram are covalently linked by a  $\text{C}_4$ -diacid moiety in order to increase the efficiency of pore formation [11, 18, 19]. The introduction of a lipophilic capping of the hydrophilic gramicidin C terminus using the *t*-Butyldiphenylsilyl (TBDPS) group leads to THF-gram-TBDPS. The syntheses of THF-gram and THF-gram-TBDPS were carried out by segment coupling in solution as described earlier [13, 23]. All synthetic ion channels were purified by RP-HPLC (Figures 2A and 2C) and characterized by  $^1\text{H-NMR}$  and MS. In addition, a linked gA-TBDPS was synthesized to explore the effect of the covalent linkage in more detail [23].

In this study, trabecular meshwork cells of the eye were chosen as the biological target for the implantation of the synthetic ion channels [24]. The trabecular meshwork is a smooth muscle-like tissue which is involved in the regulation of the intraocular pressure, a major risk factor in the etiology of glaucoma [25, 26]. Our goal was to study the response of the living cells to the different synthetic ion channels, e.g., the effect on the native membrane conductance or the response time. The functional analysis of the synthetic ion channels in planar lipid bilayers was addressed first. Second, the response of the trabecular meshwork cells to the synthetic ion channels was studied by patch-clamp techniques.

## Results

### Single-Channel Recordings in Artificial Lipid Bilayers

Conductance experiments with THF-gram were performed in artificial phospholipid bilayers of the black-lipid type prepared from soybean lecithin and *n*-decane. In these recordings, THF-gram showed characteristic single-channel events (Figure 2B). Several different sub-

\*Correspondence: o.strauss@uke.uni-hamburg.de

<sup>4</sup>Current address: Fachbereich Chemie, Philipps-Universität Marburg, 35032 Marburg, Germany.

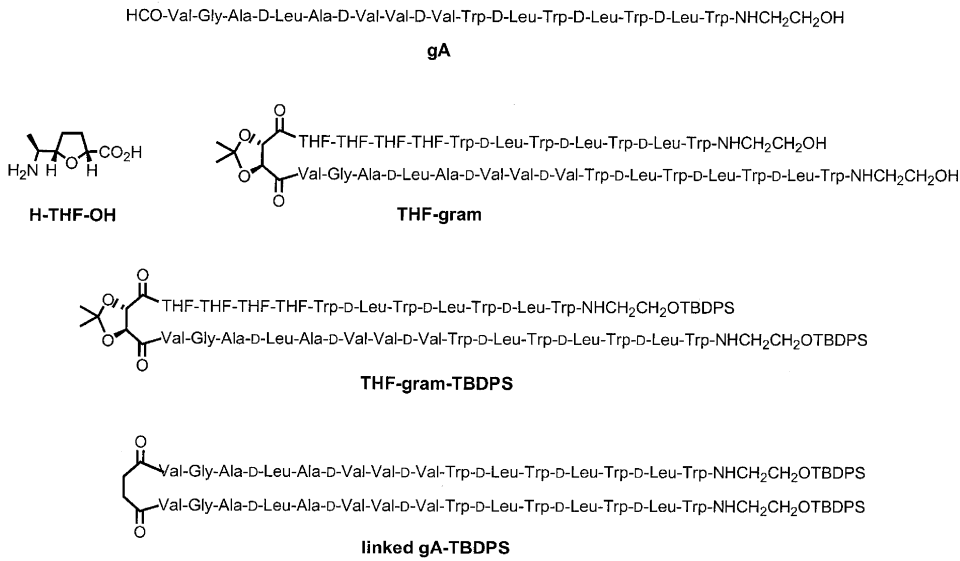


Figure 1. Structures of gA, THF-Gram, THF-Gram-TBDPS, and Linked gA-TBDPS

conductance levels were observed, indicating more than one-channel active conformation. The amplitude histogram for K<sup>+</sup> currents of THF-gram shows that the two highest level (2.3 and 2.5 pA) contribute the most to the overall membrane conductance (see Supplemental Data). Thus, these levels were used for further evaluation. Concerning ion selectivity, THF-gram showed a weak ion preference in the order NH<sub>4</sub><sup>+</sup> > Cs<sup>+</sup> > K<sup>+</sup> >

Na<sup>+</sup> in a range of 2.6: 1 for the conductance and 10: 1 for the permeability between NH<sub>4</sub><sup>+</sup> and Na<sup>+</sup> (see Supplemental Data). THF-gram-TBDPS showed a channel behavior similar to THF-gram. The channel-opening times for THF-gram and for THF-gram-TBDPS were shorter compared to linked-gA-TBDPS (see below). Several conductance levels (Figure 2D) and a weak ion selectivity NH<sub>4</sub><sup>+</sup> > Cs<sup>+</sup> > K<sup>+</sup> > Na<sup>+</sup> were observed for THF-

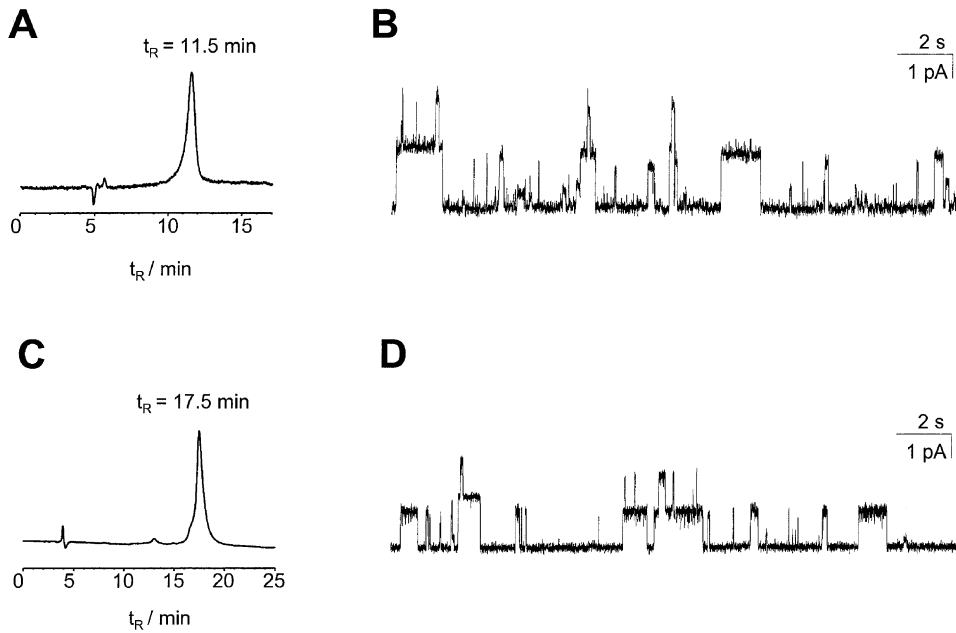


Figure 2. HPL-Chromatograms and Single-Channel Recordings in Artificial Bilayers (BLM) of Synthetic Ion Channels  
(A) HPL-chromatogram of THF-gram. Rainin Dynamax C-8 column: A, H<sub>2</sub>O; B, MeOH; 85%–100% B over 25 min.  
(B) Single-channel current trace of THF-gram.  
(C) HPL-chromatogram of THF-gram-TBDPS. Macherey-Nagel Nucleosil 100-5 C-8 column: A, H<sub>2</sub>O; B, MeOH; 85%–100% B over 25 min.  
(D) Single-channel current trace of THF-gram-TBDPS. Single-channel currents were recorded in soybean lecithin membranes: 1 M KCl; 100 mV; 20°C; c = 10<sup>-8</sup> M.

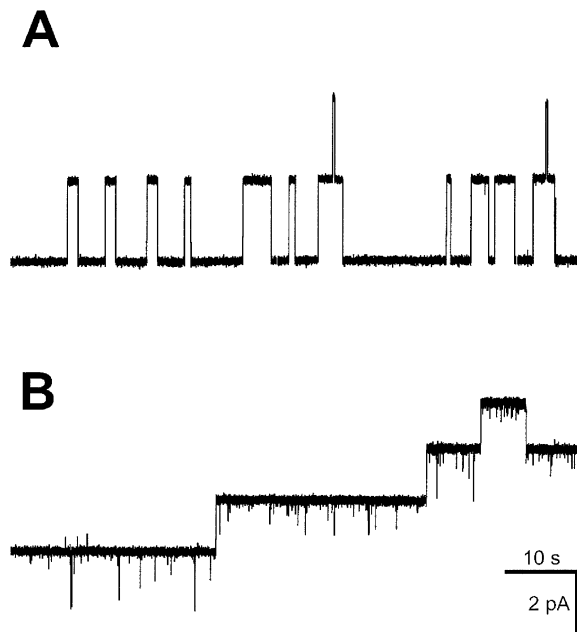


Figure 3. Comparison of Single-Channel Properties from gA and Linked-gA-TBDPS

Typical single-channel currents in BLM soybean lecithin membranes in 1 M KCl at a membrane potential of 100 mV in the presence of gA ( $10^{-12}$  M; [A]) and linked-gA-TBDPS ( $10^{-14}$  M; [B]). For an interesting explanation for the flickering observed with linked-gA-TBDPS, see [31].

gram-TBDPS. However, with THF-gram-TBDPS the values for the highest conductance levels were about 10%–40% lower for the different cations and the permeability ratios less pronounced than for THF-gram. In further experiments, we recorded the single-channel characteristics of gA and linked-gA-TBDPS in black-lipid membranes (Figure 3). gA displayed the known, stochastic appearance of single-channel currents, which correspond to the association/dissociation of channel-active gramicidin dimers [5]. Linked-gA-TBDPS showed a completely different pattern of single-channel activity. The single-channel events stayed in the open configuration for more than 30 min experimental time. Some very short and incomplete closures were occasionally observed. However, the linked-gA-TBDPS showed a smaller single-channel conductance resulting from the local hydrophobic disturbance of the  $\text{CH}_2\text{CH}_2$ -linker and the steric influence of the bulky TBDPS-group.

#### Patch-Clamp Control Experiments

Patch-clamp recordings were performed in the whole-cell configuration. This patch-clamp configuration allowed stable recordings of membrane conductance for 15–20 min with cells of the trabecular meshwork. Under control conditions (using Ringer bath solution and standard-pipette solution), the overall current density of the membrane conductance of trabecular meshwork was  $4.0 \pm 0.5$  pA pF $^{-1}$  ( $n = 69$ ). The currents were characterized by the outwardly rectifying potassium currents through the maxi-K  $\text{K}^+$  channel, which provides the main membrane conductance in these cells [24, 25]. After 10 min application of 0.5% DMSO, the current density was

$92.2 \pm 9\%$  of the values measured before application of DMSO ( $n = 3$ ), and the reversal potential was changed by  $+1 \pm 1.5$  mV ( $n = 3$ ). After 10 min application of 0.5% methanol to the bath solution, the current density was  $97.3 \pm 11.3\%$  of the values measured before application of methanol ( $n = 3$ ), and the reversal potential was changed by  $-0.53 \pm 2.8$  mV ( $n = 3$ ). The values observed after application of methanol or DMSO were not significantly different from the control values.

#### Effects of THF-Gram and THF-Gram-TBDPS on Trabecular Meshwork Cells

Application of  $10^{-6}$  M THF-gram led to an increase in the membrane conductance of trabecular meshwork cells (Figure 4). This was observed in 80% of all investigated cells.  $103 \pm 26$  s ( $n = 7$ ) after beginning of the compound application, the hyperpolarization-induced inward currents and the depolarization-induced outward currents started to increase. Usually, after 10–15 min in the presence of the substance the current amplitudes reached maximal values. At that point, the overall density of membrane currents was increased by  $5.8 \pm 2.0$  pApF $^{-1}$  ( $n = 7$ ; Figure 5A) when using  $\text{K}^+/\text{Na}^+$  as charge carriers (Ringer solution as bath solution and standard pipette solution). Under these conditions, the reversal potential of the membrane currents was shifted by  $+12.1 \pm 3.4$  mV ( $n = 10$ ) toward more positive values (Figure 5B). The effect of THF-gram was concentration dependent between  $10^{-8}$  M and  $10^{-6}$  M. An asymmetric change of the outward/inward current was observed (Figure 5C). The increase in the outward current density (by  $4.7 \pm 1.6$  pApF $^{-1}$ ;  $n = 7$ ;  $10^{-6}$  M of THF-gram) was larger than the increase in the inward current density (by  $1.1 \pm 0.4$  pApF $^{-1}$ ;  $n = 7$ ;  $p = 0.049$ ). The asymmetric behavior of the synthetic channels in the living cells may result from the asymmetry of the biological membrane. In symmetrical bilayers, no asymmetry was observed. When using  $\text{Cs}^+$  as the main charge carrier ( $\text{Cs}$ -Ringer in the bath and  $\text{Cs}$ -pipette solution in the pipette; Figure 5D) application of  $10^{-6}$  M of THF-gram increased the overall current density by  $17.5 \pm 2.6$  pApF $^{-1}$  ( $n = 5$ ). The current density measured with  $\text{Cs}^+$  as the main charge carrier was significantly higher than with  $\text{Na}^+/\text{K}^+$  as charge carriers ( $p = 0.005$ ).

Upon addition of THF-gram-TBDPS at a concentration of  $10^{-6}$  M, only 30% of all investigated cells reacted with an increase in the membrane conductance in the 15–20 min time frame for stable recordings in the whole-cell configuration (Figure 6). We therefore prolonged the substance exposure time of the cells. In these experiments, the cells were incubated for 1 hr in Ringer containing  $10^{-6}$  M with THF-gram-TBDPS (Figure 6D). Then we compared current density and reversal potential of membrane currents of cells treated under these conditions with cells which had been incubated only with DMSO. In cells treated with THF-gram-TBDPS for 1 hr, 85% of cells showed a positive response regarding increase of conductance. Using  $\text{K}^+/\text{Na}^+$  as charge carriers, THF-gram-TBDPS increased the overall current density by  $6 \pm 2.4$  pApF $^{-1}$  ( $n = 7$ ; see Supplemental Data). The reversal potential was shifted by  $+21 \pm 4.5$  mV ( $n = 7$ ) toward more positive values. In the incubation

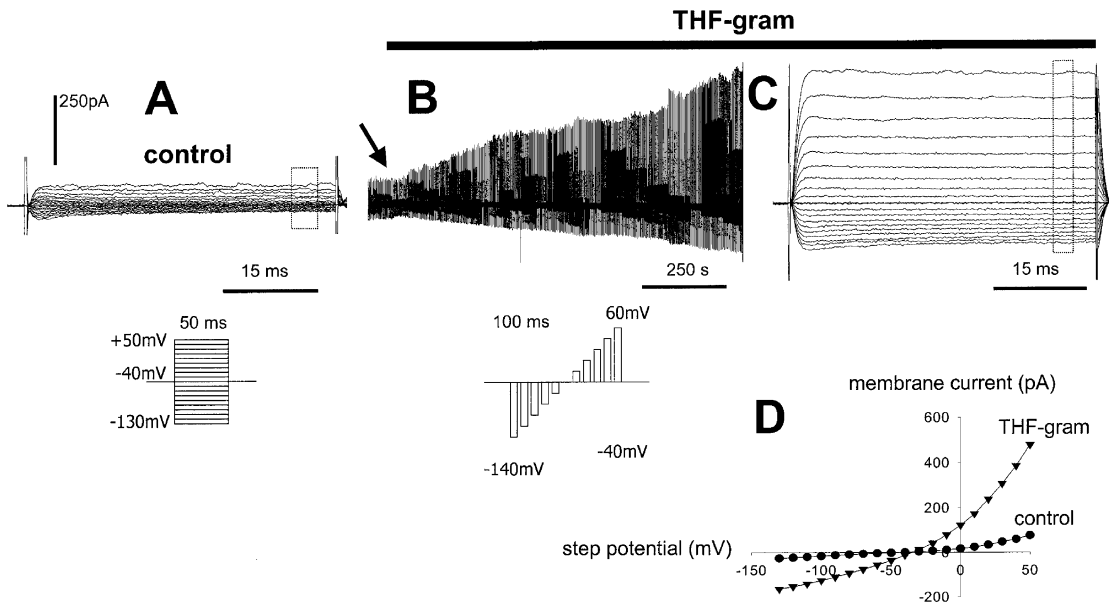


Figure 4. Response of Trabecular Meshwork Cells to THF-Gram

(A) Whole-cell currents of a trabecular meshwork cell under control conditions. The cell was clamped to  $-40$  mV and electrically stimulated by the protocol that is shown below.  
 (B) Change in the membrane conductance of a trabecular meshwork cell by application of THF-gram ( $10^{-6}$  M). The membrane currents were continuously recorded at a holding potential of  $-40$  mV. To monitor the membrane conductance, the cell was stimulated every 2.5 s by the protocol shown below. The black bar indicates the time for which the cells were exposed to THF-gram; the arrow indicates the moment when application started.  
 (C) Membrane currents of the trabecular meshwork cell in the presence of THF-gram. The currents were stimulated by the protocol as shown in (A). The recording was started after finishing the recording shown in (B).  
 (D) Current/voltage of the currents shown in (A) and (C). The steady-state currents (estimated in the frames shown in [A] and [C]) were plotted against the potential of the electrical stimulation.

experiments, the cells showed an increase in overall current density of  $4.7 \pm 1.7$  pApF $^{-1}$  ( $n = 35$ ) versus the DMSO controls and a reversal potential that was  $14.6 \pm 6.3$  mV ( $n = 35$ ) more positive than the DMSO-treated controls. All these effects were observed in the concen-

tration range between  $10^{-7}$  to  $10^{-6}$  M. When comparing the increase in depolarization-induced outward current density with hyperpolarization-induced inward current density, no significant difference was observed (outward  $3.9 \pm 1.9$  pApF $^{-1}$ ,  $n = 7$  versus inward  $3.5 \pm 2.1$  pApF $^{-1}$ ,

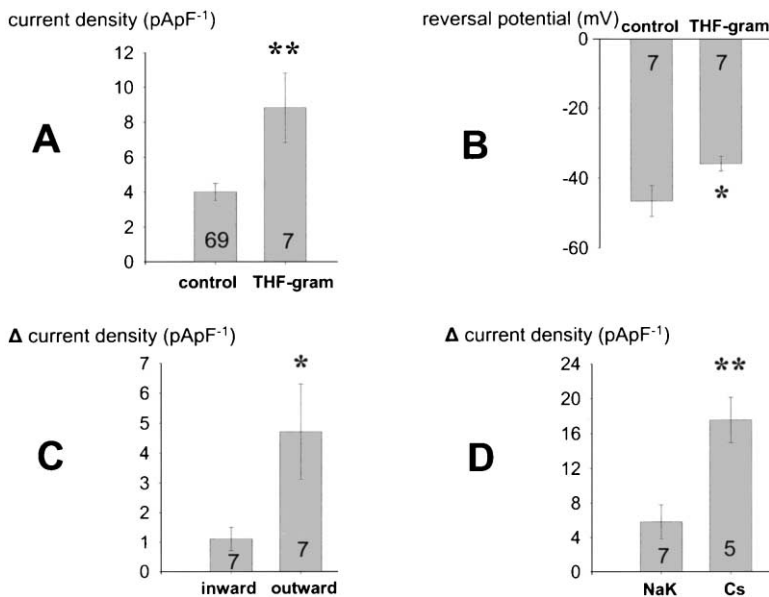


Figure 5. Summary of the Effects of THF-Gram on the Membrane Conductance of Trabecular Meshwork Cells

(A) Increase in the overall current density ( $c = 10^{-6}$  M).  
 (B) Effect on the reversal potential of trabecular meshwork cells.  
 (C) Comparison of increase in outward current and inward current density.  
 (D) Comparison of induced increase in current density when  $\text{Na}^+$  and  $\text{K}^+$  were used as charge carriers (physiological intracellular  $\text{K}^+$  concentration and physiological extracellular  $\text{Na}^+$  concentration) with the increase in current density when  $\text{Cs}^+$  was used as main charge carrier (intra- and extracellular solutions contained mainly  $\text{Cs}^+$  as monovalent cations).

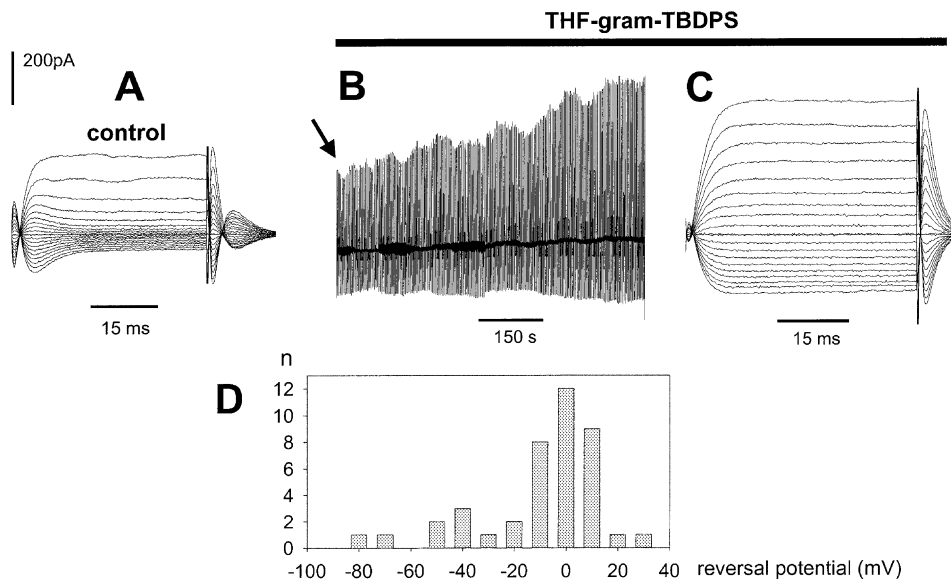


Figure 6. Effect of Application of THF-Gram-TBDPS to Trabecular Meshwork Cells.

(A) Whole-cell currents of a trabecular meshwork cell under control conditions. The cell was clamped to  $-40$  mV and electrically stimulated by the protocol shown in the lower panel of Figure 4A.

(B) Change in the membrane conductance of a trabecular meshwork cell by application of THF-gram-TBDPS ( $c = 10^{-6}$  M) which has been observed in 30% of all cells. The membrane currents were continuously recorded at a holding potential of  $-40$  mV. To monitor the membrane conductance, the cell was stimulated every 2.5 s by the protocol shown in the lower panel of Figure 4B. The black bar indicates the time for which the cells were exposed to the synthetic ion channel; the arrow indicates the moment when application was started.

(C) Membrane currents of the trabecular meshwork cell in the presence of THF-gram-TBDPS. The currents were stimulated by the protocol shown in the lower panel of Figure 4A; the recording was started after finishing the recording shown in Figure 4B.

(D) Results of 1 hr incubation of trabecular meshwork cells with THF-gram-TBDPS. The reversal potentials were measured and grouped into the voltage ranges of  $-80$ – $(-70)$  mV,  $-70$ – $(-60)$  mV,  $-60$ – $(-50)$  mV, following this pattern to  $20$ – $30$  mV. The number of cells showing currents with reversal potentials in these groups was plotted against the corresponding voltage ranges. Most cells showed a reversal potential between  $-10$  mV and  $+10$  mV after 1 hr incubation.

$n = 7$ ; see Supplemental Data). Using  $\text{Cs}^+$  as the main charge carrier, THF-gram-TBDPS increased the overall density of membrane currents by  $10.5 \pm 3.0$  pApF $^{-1}$  ( $n = 4$ ).

#### Effect of Linked-gA-TBDPS and gA on Trabecular Meshwork Cells

In order to elucidate the influence of the covalent linkage of the two gA motifs in more detail, the responses of the cells to gA and linked-gA-TBDPS were studied by patch-clamp analysis.  $115 \pm 20$  s ( $n = 6$ ) after beginning to expose the cells to gA ( $10^{-6}$  M), the membrane conductance started to increase (Figure 7). Maximum response of the cells was observed after 10 min exposure time. When using  $\text{K}^+/\text{Na}^+$  as charge carriers, gA increased the overall current density by  $23.8 \pm 3.7$  pApF $^{-1}$  ( $n = 8$ ) and shifted the reversal potential by  $+22.6 \pm 8$  mV ( $n = 8$ ) toward more positive values. With these ions as charge carriers, the overall conductance increased by  $1.7 \pm 0.3$  pA per s ( $n = 6$ ). The increase in the membrane conductance and shift in the reversal potential moved the current to clamp the membrane potential on to more negative values. This can be seen as drift in the baseline during the voltage-clamp experiment. The outward current density was increased by  $13.5 \pm 1.9$  pApF $^{-1}$  ( $n = 8$ ), whereas the inward current density was increased by  $10.2 \pm 1.9$  pApF $^{-1}$  ( $n = 8$ ). Both values are not statistically different ( $p = 0.24$ ). The level of the gA-induced

changes in the membrane conductance was always high enough to lead to cell destruction after several minutes.

Application of linked-gA-TBDPS gave a much faster and more effective response of the trabecular meshwork cells (Figure 7). Linked-gA-TBDPS started to show an effect at  $10^{-14}$  M. Application of  $10^{-12}$  M of linked-gA-TBDPS increased the overall current density by  $8.6 \pm 1.9$  pApF $^{-1}$  ( $n = 5$ ) and shifted the reversal potential of currents toward more positive potentials by  $+11.4 \pm 4$  pApF $^{-1}$  ( $n = 5$ ). The effect was measurable  $33.3 \pm 7.2$  s ( $n = 6$ ) after the beginning of exposure, and the membrane conductance rose by  $5.0 \pm 1.2$  pA per second ( $n = 6$ ). Maximum response of the cells was observed after 2 min of exposure time. Also, in this case the increase in the membrane conductance was high enough so that the application led to a drift in the baseline of the holding current during the voltage-clamp experiment. No differences between increase in inward and outward current density were observed with linked-gA-TBDPS (see Supplemental Data). Using  $\text{Cs}^+$  as main charge carrier, the overall current density was increased by  $18.4 \pm 2.4$  pApF $^{-1}$  ( $n = 3$ ).

#### Discussion

Both synthetic ion channels, THF-gram and THF-gram-TBDPS, led to an increase in the membrane conduc-

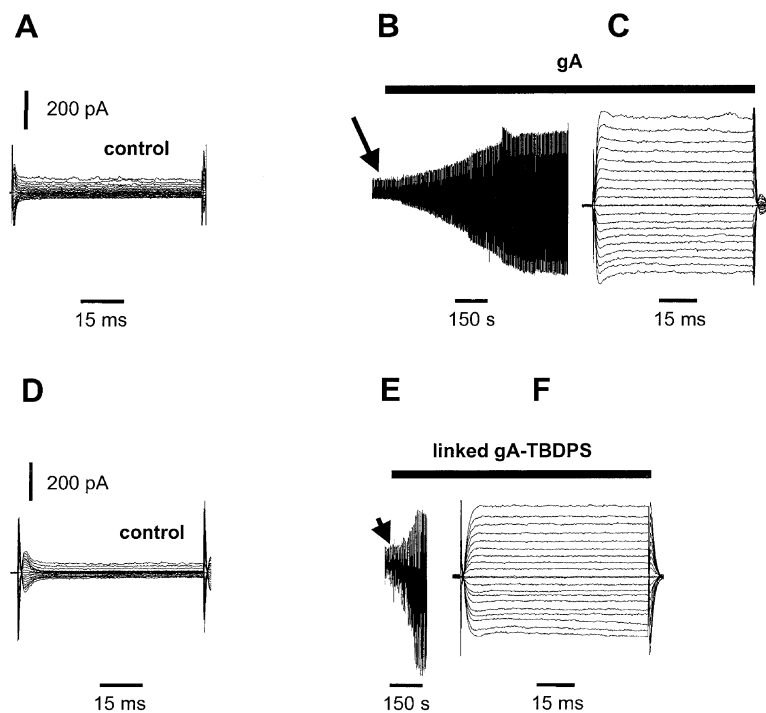


Figure 7. Response of Trabecular Meshwork Cells to gA and Linked-gA-TBDPS

(A) Whole-cell currents of a trabecular meshwork cell under control conditions. The cell was clamped to  $-40$  mV and electrically stimulated by the protocol shown in the lower panel of Figure 4A.

(B) Change in the membrane conductance of a trabecular meshwork cell by application of gA ( $10^{-6}$  M). The membrane currents were continuously recorded at a holding potential of  $-40$  mV. To monitor the membrane conductance, the cell was stimulated every 2.5 s by the protocol shown in the upper panel of Figure 4B. The black bar indicates the time for which the cells were exposed to gA; the arrow indicates the moment when application was started.

(C) Membrane currents of the trabecular meshwork cell in the presence of gA. The currents were stimulated by the protocol shown in the lower panel of Figure 4A; the recording was started after finishing the recording shown in (B).

(D) Whole-cell currents of a trabecular meshwork cell under control conditions. The cell was clamped to  $-40$  mV and electrically stimulated by the protocol shown in the lower panel of Figure 4A.

(E) Change in the membrane conductance of

a trabecular meshwork cell by application of linked-gA-TBDPS ( $10^{-14}$  M). The membrane currents were continuously recorded at a holding potential of  $-40$  mV. To monitor the membrane conductance, the cell was stimulated every 5 s by the protocol shown in the lower panel of Figure 4B. The black bar indicates the time for which the cells were exposed to linked-gA-TBDPS; the arrow indicates the moment when application was started.

(F) Membrane currents of the trabecular meshwork cell in the presence of linked-gA-TBDPS. The currents were stimulated by the protocol shown in the lower panel of Figure 4A; the recording was started after finishing the recording shown in (E).

tance of cultured trabecular meshwork cells, which added to the membrane conductance provoked by naturally expressed ion channels, assuming that the behavior of the biological channels remained mostly unchanged. With THF-gram, the additional current density was approximately two times higher than the current density of naturally expressed ion channels under control conditions. This response began at a concentrations of  $10^{-8}$  M and was saturated at a concentration of  $10^{-7}$  M. This range is too small to reasonably estimate a concentration dependence and should be taken into account for further studies. The increase in conductance was compatible with the vital functions of the biological system. The cells could survive an incubation for 1 hr with THF-gram-TBDS in its maximal effective concentration. In contrast, application of the same concentration of gA led, after an initial increase in the membrane conductance, to the fast destruction of all cells.

The cells responded to the application of THF-gram with a shift of the reversal potential toward more positive values but still remained in a negative voltage range. Remarkable is the asymmetry for the increase of the inward/outward current density. The THF-gram cation channel induced higher current densities in outward direction than in inward direction. Possible explanations are an asymmetric function of the compound in the membrane in combination with an asymmetric incorporation into the membrane or an influence of complex ionic solutions. Further studies in planar lipid bilayers should distinguish between both possibilities and clarify

this interesting point. The current density in trabecular meshwork cells was dependent on the type of cation used as the main charge carrier. When using  $\text{Cs}^+$  instead of  $\text{Na}^+/\text{K}^+$ , we observed significantly higher current densities in the presence of THF-gram. This is in agreement with the higher  $\text{Cs}^+$  conductance ( $\text{Cs}^+ : \text{K}^+ : \text{Na}^+ = 2.0 : 1.4 : 1$ ) observed in the planar-lipid bilayer experiments.

The cell response of THF-gram-TBDPS was less pronounced compared to THF-gram. One reason could be the lower solubility of THF-gram-TBDPS in an aqueous environment, which may impede the transport to the cell. On the other side, the big lipophilic TBDPS groups at the C termini of the compound may interact with the biological membrane to delay the formation of channel-active conformation. The changes in the overall current density were in the same range as the changes induced by THF-gram.

The comparison of the cell response to gA and linked-gA-TBDPS shows that the covalent linkage, which results in the transition from a bimolecular to a monomolecular channel, leads to a faster response time in the biological system. With linked-gA-TBDPS, the effect on the membrane conductance occurred at concentrations beginning with  $10^{-14}$  M, while comparable effects with gA were observed at concentrations of  $10^{-8}$  M. The covalent linkage in linked-gA-TBDPS avoids the dimer association step necessary for gA to form active channels, leading to a faster and more sensitive cell response. Linked-gA-TBDPS shows a larger effect on cells than THF-gram and THF-gram-TBDPS. A possible ex-

planation is the conformational flexibility of the THF amino acid, which can give rise to nonchannel active conformations. This is the main reason for the smaller dwell times and the existence of several conductance levels for THF-gram. However, the mostly open channel in linked-gA-TBDPS causes a control problem, while the conformational flexibility of THF-gram offers the chance for conformational switching to gate the channel.

#### Possible Applications of Synthetic Ion Channels

Synthetic ion channels are not only valuable tools to study the mechanism of biological ion transport. Currently, the use of gA-channel-based systems for nanosensors is an active field [27]. Our long-term goal is to develop ion channels as drugs for therapeutical approaches. The above-discussed observations demonstrate that compounds such as THF-gram represent a basis to develop synthetic ion channels as a drug for therapy. The substances alter the membrane conductance without destroying the cell. Furthermore, the additional membrane conductance can be influenced by structural modifications. The next step should address the change of the functional properties of the tissue. For this purpose, measurements of the contractility of trabecular meshwork strips under the influence of THF-gram are planned. In these experiments, one could expect an increase in the contraction force developed by the trabecular network tissue. THF-gram leads to a mild depolarization of the cells, which in turn should increase the contraction force of the trabecular meshwork, a smooth muscle-like tissue.

To further develop compounds such as THF-gram toward therapeutical uses, two main problems have to be solved. First, the substance must show a defined ion selectivity. In order to develop an antiglaucoma drug, the ion channel should have a  $K^+$  selectivity, which leads to hyperpolarization and a decrease of the contraction force. As we showed in previous studies, this effect increases the outflow rate of the aqueous humor in the eye with a subsequent reduction of intraocular pressure. The reduction of intraocular pressure is a priority goal in the treatment of glaucoma. The second problem is the cell-specific targeting of the drug. Basically, THF-gram will incorporate in every cell membrane which is exposed to the drug. This problem could be solved, e.g., by formation of an antibody-THF-gram conjugate.

#### Significance

This study of synthetic channels in living cells is a first step toward the long-term goal of the controlled channel implantation into specific tissues. So far, synthetic ion channels were mainly used to study mechanisms of ion transport in artificial lipid bilayer membranes [29, 30]. This is the first study that describes effects of synthetic ion channels on membrane conductance of living trabecular meshwork cells. Application of THF-gramicidin-hybrid channels increased the membrane conductance in association with a mild depolarization of the cell. This membrane conductance adds to the naturally expressed membrane conductance and displays characteristics of weak-Eisenman

I selective cation channels. The additional membrane conductance showed current densities comparable to naturally expressed conductances and did not lead to cell destruction. The asymmetry of the induced inward/outward currents points to an asymmetric function of the THF-hybrid channels in the biological membrane. With these characteristics, THF-gramicidin-hybrid cation channels represent a good basis for further development in designing substances with defined properties such as ion selectivity or tissue-specific control of ion channel activity.

#### Experimental Procedures

##### Substances

Media and cell culture supplements were purchased from Biochrom (Berlin, Germany). Chemicals were purchased from Sigma (Munich, Germany), Serva (Heidelberg, Germany), Merck (Darmstadt, Germany). Gramicidin A (>90% HPLC) came from Fluka. THF-gram, THF-gram-TBDPS, and linked-gA-TBDPS were synthesized as described before [12, 22].

##### Purification and Purity Control of the Synthetic Ion Channels

The purification procedure for THF-gram and THF-gram-TBDPS consisted of flash column chromatography (FC) on silica gel 60 (230-400 mesh) from Merck (Darmstadt, Germany) or preparative thin layer chromatography (TLC) on silica gel 60 F-245 glass plates,  $200 \times 200 \times 1$  mm, Merck (Darmstadt, Germany), followed by preparative reversed phase HPLC ( $250 \times 20$  mm column, 15 mL/min) and gel permeation chromatography (GPC) on Sephadex LH-20 from Sigma (Munich, Germany),  $CHCl_3/MeOH$  1:1. THF-gram: preparative TLC ( $CHCl_3/MeOH$  10:1), HPLC (Rainin Dynamax C-8 column, A =  $H_2O$ , B = MeOH, 85 to 100% B over 25 min), GPC. THF-gram-TBDPS: FC ( $CHCl_3/MeOH$  30:1 to  $CHCl_3/EtOH$  5:1), HPLC (Machrey-Nagel Nucoasil 100-5 C-8 column, A =  $H_2O$ , B =  $CH_3CN/i-PrOH$  2:1, 80% B isocratic), GPC. Linked-gA-TBDPS was purified as described before [22]. gA was used without further purification. All purification steps were controlled by analytical HPLC (final purity: >95%, HPLC chromatograms see Figure 2) and single-channel recordings on BLM.

##### Recordings with Artificial Bilayers of the Black Lipid Type

Planar lipid membranes were prepared by painting a solution of soybean lecithin (40%; Avanti Polar Lipids, Alabaster, AL) in *n*-decane (25 mg/ml) over the aperture of a polystyrene cuvette with a diameter of 0.15 mm [28]. All experiments were performed at ambient temperature. The electrolyte solutions at a concentration of 1 M each were unbuffered. The probes, dissolved in methanol, were added to the *trans* side of the cuvette (containing the reference electrode), resulting in a bath concentration of 0.01–0.03  $\mu M$  (THF-gram and THF-gram-TBDPS) or 1 pM (linked-gA-TBDPS and gA). Current detection and recording was performed with a patch-clamp amplifier Axopatch 200, a Digidata A/D converter, and pClamp6 software (Axon Instruments, Foster City, MA). The acquisition frequency was 5 kHz. The data were filtered with an analog filter at 50 Hz for further analysis.

##### Cell Culture

Primary cultures of bovine trabecular meshwork were established as described previously [24–26]. Bovine eyes were obtained from a local slaughterhouse. Short, small pieces of trabecular meshwork were isolated from the eyes and placed under a glass coverslip lying in a Petri dish. The cultures were maintained in 5%  $CO_2$  in air at 37°C. Twice a week, the cultures were fed with Dulbecco's modified Eagle's minimal essential medium (DMEM) supplemented with 10% fetal calf serum, 100 U/ml penicillin, and 100  $\mu g/ml$  streptomycin. The cultures were passaged using the trypsin/EDTA method and grown to confluent monolayers.

##### Patch-Clamp Recordings

Membrane currents were measured using the whole-cell configuration of the patch-clamp technique [2]. For recordings from single

cells, monolayers of the third passage were dispersed by enzymatic treatment with trypsin for 3 min into a single-cell suspension. The cells were allowed to settle down on glass coverslips for 30 min. Glass coverslips with cells were then placed into a perfusion chamber for patch-clamp recordings which is mounted onto the stage of an inverted microscope. The patch-clamp recordings were performed at room temperature. During patch-clamp recordings, the cells were superfused with the bath solution Ringer containing (mM) 141 NaCl, 4 KCl, 1.7 CaCl<sub>2</sub>, 0.9 MgCl<sub>2</sub>, 10 HEPES, 5 glucose (pH 7.4) adjusted with Tris. To compare the conductance of artificially made ion channels between Na<sup>+</sup>, K<sup>+</sup>, and Cs<sup>+</sup>, the following bath solution (Cs-Ringer) was used (mM): 131 CsCl, 10 NaCl, 4 KCl, 1.7 CaCl<sub>2</sub>, 0.9 MgCl<sub>2</sub>, 10 HEPES, 5 glucose (pH 7.4) adjusted with Tris. Patch pipettes with a pipette resistance of 3–5 MΩ were pulled from borosilicate glass tubes using a Zeitz DMZ Universal Puller (Zeitz Augsburg, Germany). Patch pipettes were filled with a standard pipette solution containing (mM) 119 K-glutamate, 10 NaCl, 1 K<sub>2</sub>HPO<sub>4</sub>, 0.9 MgSO<sub>4</sub>, 10 HEPES, 0.5 CaCl<sub>2</sub>, 5.5 EGTA (pH 7.2) adjusted with Tris. The final concentration of Ca<sup>2+</sup> in the pipette solution was 12 nM to avoid the activation of Ca<sup>2+</sup>-dependent K<sup>+</sup> channels. For experiments to study the conductance with Cs<sup>+</sup> as the main charge carrier, Cs-pipette solution was used, where monovalent cation ions were replaced with Cs<sup>+</sup> (mM) 119 Cs-methanesulfonate, 10 NaCl, 0.9 MgSO<sub>4</sub>, 10 HEPES, 0.5 CaCl<sub>2</sub>, 5.5 EGTA (pH 7.2) adjusted with Tris. Synthetic ion channels were used as DMSO- or methanol-based stock solution. The substances were added to the bath solution so that the final concentration of DMSO or methanol did not exceed 0.5%.

Whole-cell currents were measured using an EPC 9 patch-clamp amplifier (HEKA Electronics, Lambrecht, Germany) in conjunction with an AT-compatible computer. Control of the patch-clamp amplifier, electrical stimulation, data collection, and analysis were performed using the TIDA for Windows software (HEKA). Currents were filtered with a 2.9 kHz lowpass Bessel filter. The cells showed a membrane capacitance of 60.3 ± 5.4 pF (n = 69) and an access resistance of 10.1 ± 0.6 MΩ (n = 69). The access resistance was compensated to 5 MΩ.

#### Electrical Stimulation and Determination of Current Density

To study the membrane conductance, the cells were electrically stimulated using two different pulse protocols. The first type of stimulation was used to evaluate current/voltage plots (Figure 4A). Here, the cells were depolarized from the holding potential of -40 mV with nine voltage steps of 50 ms duration and 10 mV increasing amplitude and hyperpolarized with nine voltage steps of 50 ms duration and -10 mV decreasing amplitude. The other type of stimulation was used to monitor acute effects (Figure 4B). For this purpose, the membrane currents were continuously measured at a holding potential of -40 mV for 125 s. During this time, the cell was stimulated every 2.5 s by five voltage steps to the potentials -140 mV, -120 mV, -100 mV, -80 mV, and -60 mV (each voltage step lasted 100 ms) to hyperpolarize the cell, followed by five voltage steps to the potentials -20 mV, 0 mV, +20 mV, 40 mV, and +60 mV (each voltage step lasted 100 ms) to depolarize the cell. The sampling rate during this stimulation protocol was 100 Hz. To calculate the inward current density, the steady current at -140 mV was measured and normalized to the cell capacitance, which is a measure of the cell size. To calculate the outward current density, the current at +60 mV was measured and normalized to the cell capacitance. The overall current density was calculated as the sum of the inward and outward current density. To describe the effects of synthetic ion channels, the difference of current density before application and in the presence of the compound is given.

#### Statistical Analysis

If not otherwise stated, all data are given as mean ± SEM. N refers to the number of experiments; each experiment was performed with one cell. Analyses for significance were performed using Student's t test. Statistical significance was considered at p values lower than 0.05.

#### Supplemental Data

Supplemental Data for this article includes an amplitude histogram for THF-gram in BLM; a current/voltage plot for THF-gram using

various cations as charge carriers; changes in current density for patch-clamp experiments with THF-gram-TBDPS; and changes in current density for patch-clamp experiments with gA and linked-gA-TBDPS. Please write to chembiol@cell.com for a PDF.

#### Acknowledgments

The authors want to thank Dr. Friederike Stumpff for helpful discussions and Marianne Boxberger for expert technical assistance. The work is supported by VW-Foundation grant I/75 310.

Received: July 24, 2002

Revised: October 16, 2002

Accepted: November 15, 2002

#### References

1. Ackerman, M.J., and Clapham, D.E. (1997). Ion channels-basic science and clinical disease. *N. Engl. J. Med.* **336**, 1575–1586.
2. Hamill, O.P., Marty, A., Neher, E., Sakmann, B., and Sigworth, F.J. (1981). Improved patch-clamp techniques for high-resolution current recording from cells and cell-free membrane patches. *Pflügers Arch.* **391**, 85–100.
3. Zhou, Y., Morais-Cabral, J.H., Kaufman, A., and MacKinnon, R. (2001). Chemistry of ion coordination and hydration revealed by a K<sup>+</sup> channel-Fab complex at 2.0 Å resolution. *Nature* **414**, 43–48.
4. Jiang, Y., Lee, A., Chen, J., Cadene, M., Chait, B.T., and MacKinnon, R. (2002). Crystal structure and mechanism of a calcium-gated potassium channel. *Nature* **417**, 515–522.
5. Chadwick, D.J., and Cardew, G. (1999). Gramicidin and Related Ion Channel-Forming Peptides (Chichester, UK: Wiley).
6. Wallace, B.A. (1998). Recent advances in the high resolution structures of bacterial channels. *Gramicidin A. J. Struct. Biol.* **121**, 123–141.
7. Gokel, G.W., Ferdani, R., Liu, J., Pajewski, R., Shabany, H., and Uetrecht, P. (2001). Hydratable channels: models for transmembrane, cation-conducting transporters. *Chemistry* **7**, 33–39.
8. Yoshino, N., Satake, A., and Kobuke, Y. (2001). An artificial ion channel formed by a macrocyclic resorcin[4]arene with amphiphilic cholic acid ether groups. *Angew. Chem. Int. Ed. Engl.* **40**, 457–459.
9. Ghadiri, M.R., Granja, J.R., and Buehler, L.K. (1994). Artificial transmembrane ion channels from self-assembling peptide nanotubes. *Nature* **369**, 301–304.
10. Baumeister, B., Sakai, N., and Matile, S. (2000). Giant artificial ion channels formed by self-assembled, cationic rigid-rod beta-barrels. *Angew. Chem. Int. Ed. Engl.* **39**, 1955–1958.
11. Stankovic, C.J., and Schreiber, S.L. (1991). Molecular design of transmembrane ion channels. *Chemtracts: Org. Chem.* **4**, 1–19.
12. Rottenberg, H., and Koeppel, R.E. (1989). Stimulation of cation transport in mitochondria by gramicidin and truncated derivatives. *Biochemistry* **28**, 4361–4367.
13. Schrey, A., Vescovi, A., Knoll, A., Rickert, C., and Koert, U. (2000). Synthesis and functional studies of a membrane-bound THF-gramicidin cation channel. *Angew. Chem. Int. Ed. Engl.* **39**, 900–902.
14. Koeppel, R.E., and Andersen, O.S. (1996). Engineering the gramicidin channel. *Annu. Rev. Biophys. Biomol. Struct.* **25**, 231–258.
15. Woolley, G.A., Jaikaran, A.S.I., Zhang, Z., and Peng, S. (1995). Design of regulated ion channels using measurements of cis-trans isomerization in single molecules. *J. Am. Chem. Soc.* **117**, 4448–4454.
16. Arndt, H.D., Knoll, A., and Koert, U. (2001). Cyclohexylether delta-amino acids: new leads for selectivity filters in ion channels. *Angew. Chem. Int. Ed. Engl.* **40**, 2076–2078.
17. Stankovic, C.J., Heinemann, S.H., Delfino, J.M., Sigworth, F.J., and Schreiber, S.L. (1989). Transmembrane channels based on tartaric acid-gramicidin A hybrids. *Science* **244**, 813–817.
18. Urry, D.W., Goodall, M.C., Glickson, J.D., and Mayers, D.F. (1971). The gramicidin A transmembrane channel: characteristics of head-to-head dimerized (L,D) helices. *Proc. Natl. Acad. Sci. USA* **68**, 1907–1911.



19. Armstrong, K.M., Quigley, E.P., Quigley, P., Crumrine, D.S., and Cukierman, S. (2001). Covalently linked gramicidin channels: effect of linker hydrophobicity and alkaline metals on different stereoisomers. *Biophys. J.* *80*, 1810–1818.
20. Jude, A.R., Providence, L.L., Schmutzer, S.E., Shobana, S., Greathouse, D.V., Andersen, O.S., and Koeppe, R.E. (2001). Peptide backbone chemistry and membrane channel function: effects of a single amide-to ester replacement on gramicidin channel structure and function. *Biochemistry* *40*, 1460–1472.
21. Borisenko, V., Burns, D.C., Zhang, Z., and Woolley, G.A. (2000). Optical switching of ion-dipole interactions in a gramicidin channel analogue. *J. Am. Chem. Soc.* *122*, 6364–6370.
22. Schrey, A., Osterkamp, F., Straudi, A., Rickert, C., Wagner, H., Koert, U., Herrschaft, B., and Harms, K. (1999). Synthesis of enantiomerically pure amino acids containing 2,5-disubstituted THF rings in the molecular backbone. *Eur. J. Org. Chem.* *11*, 2977–2990.
23. Arndt, H.-D., Vescovi, A., Schrey, A., Pfeifer, J.R., and Koert, U. (2002). Solution phase synthesis and purification of the mini-gramicidin ion channels and a succinyl-linked gramicidin. *Tetrahedron* *58*, 2789–2801.
24. Stumpff, F., Strauss, O., Boxberger, M., and Wiederholt, M. (1997). Characterization of maxi-K-channels in bovine trabecular meshwork and their activation by cyclic guanosine monophosphate. *Invest. Ophthalmol. Vis. Sci.* *38*, 1883–1892.
25. Stumpff, F., and Wiederholt, M. (2000). Regulation of trabecular meshwork contractility. *Ophthalmologica* *214*, 33–53.
26. Wiederholt, M., Thieme, H., and Stumpff, F. (2000). The regulation of trabecular meshwork and ciliary muscle contractility. *Prog. Retin. Eye Res.* *19*, 271–295.
27. Cornell, B.A., Braach-Maksvytis, V.L., King, L.G., Osman, P.D., Raguse, B., Wieczorek, L., and Pace, R.J. (1997). A biosensor that uses ion-channel switches. *Nature* *387*, 580–583.
28. Mueller, P., and Rudin, D.O. (1967). Action potential phenomena in experimental bimolecular lipid membranes. *Nature* *213*, 603–604.
29. Cahalan, M.D., and Hall, J. (1982). Alamethicin channels incorporated into frog node of ranvier: calcium-induced inactivation and membrane surface charges. *J. Gen. Physiol.* *79*, 411–436.
30. Sidorov, V., Kotch, F.W., Abdrakhmanova, G., Mizani, R., Fetting, J.C., and Davis, J.T. (2002). Ion channel formation from a Calix[4]arene amide that binds HCl. *J. Am. Chem. Soc.* *124*, 2267–2278.
31. Armstrong, K.M., and Cukierman, S. (2002). On the origin of closing flickers in gramicidin channels: a new hypothesis. *Biophys. J.* *82*, 1329–1337.